

1

2

3 **Development of a Conceptual Warning System for Toxic Levels of *Alexandrium***

4 ***fundyense* in the Bay of Fundy based on Remote Sensing Data**

5

6 **Running page head: Remote sensing of *A. fundyense***

7

8 **List of Authors**

9 E. Devred*, J. Martin, S. Sathyendranath, V. Stuart, E. Horne, T. Platt, M.-H. Forget, and
10 P. Smith
11 E. Devred, Bedford Institute of Oceanography, Fisheries and Oceans Canada, Dartmouth,
12 NS, B2Y 4A2, Canada
13 Emmanuel.devred@dfo-mpo.gc.ca
14 J.L. Martin, Fisheries and Oceans Canada, Biological Station, St. Andrews, NB E5B 2L9,
15 Canada
16 S. Sathyendranath, Plymouth Marine Laboratory, Prospect Place, The Hoe, Plymouth,
17 PL1 3DH, United Kingdom
18 V. Stuart, Bedford Institute of Oceanography, Fisheries and Oceans Canada, Dartmouth,
19 NS, B2Y 4A2, Canada
20 E. Horne, Bedford Institute of Oceanography, Fisheries and Oceans Canada, Dartmouth,
21 NS, B2Y 4A2, Canada
22 T. Platt, Plymouth Marine Laboratory, Prospect Place, The Hoe, Plymouth,
23 PL1 3DH, United Kingdom
24 M.-H. Forget, Takuvik Joint International Laboratory, Laval University (Canada) –
25 CNRS (France), UMI3376, Département de biologie, Université Laval, Québec, QC,
26 G1V 0A6, Canada
27 P. Smith, Bedford Institute of Oceanography, Fisheries and Oceans Canada, Dartmouth,
28 NS, B2Y 4A2, Canada

29 **Abstract:** Harmful algal blooms (HABs) present a potential danger for human health and
30 commercial activities, especially in coastal regions. Observing systems increasingly rely
31 on remote sensors to monitor and possibly predict the locations and intensity of such
32 blooms. Here we present a novel approach for detecting HABs of *Alexandrium fundyense*
33 in the Bay of Fundy, Canada. *A. fundyense* is considered toxic for individuals who
34 consume shellfish when cell abundances adjacent to shellfish harvesting areas are as low
35 as 200 cells•L⁻¹, making it difficult to use direct remote sensing techniques to assess the
36 threat in the early stages of the development of the bloom. Using *in situ* *A. fundyense* cell
37 abundance measurements, together with satellite observations of sea-surface temperature
38 and the occurrence of diatom-dominated phytoplankton populations, a warning system
39 was developed based on three levels of alerts: green (low abundance of *A. fundyense*),
40 orange (possible threat of *A. fundyense*) and red (high probability of *A. fundyense*
41 concentrations that would result in shellfish toxicity above safe levels for human
42 consumption). Combined information on diatom phenology and variations in sea-surface
43 temperature are key to the timing of *A. fundyense* blooms: our data reveal that the
44 termination of the diatom spring bloom, associated with the warming of the water, can
45 trigger an increase in *A. fundyense* cell abundance. The objective criteria for a HAB
46 warning system was developed and tested in the Bay of Fundy using two different
47 datasets: one to develop the algorithm (data collected between **1998** and **2007**) and one to
48 assess its performance (data collected in 2011). The warning system is based on the
49 cautionary principle that a false negative (warning not issued when it should have been)
50 is far more serious than a false positive (warning issued when it should not have been).
51 The overall success of the algorithm when tested on the validation dataset is about 70%

52 using a threshold of 150 *A. fundyense* cells•L⁻¹, with a low occurrence of false negative
53 red alerts (<8%). The satellite-data-based warning can be used to optimize an *in situ*
54 monitoring system, which can be designed to be more intensive when the warning status
55 is orange or red. This study demonstrates that combined satellite information on
56 phytoplankton phenology and sea-surface temperature can help predict low abundances
57 of toxic *A. fundyense* cells. It also highlights the importance of an integrated approach
58 combining satellite and *in situ* observations to monitor HABs.

59

60 **1. Introduction**

61

62 Harmful algal blooms (HABs) continue to be of concern throughout the world and
63 research is focusing on the development of tools for their early detection. Toxic algae
64 occur in all phytoplankton groups, including diatoms (e.g., *Pseudo-nitzschia* spp.),
65 dinoflagellates (e.g., *Alexandrium* spp.) and cyanobacteria (e.g., *Trichodesmium* spp.).
66 This work focuses on a single species, *Alexandrium fundyense*, from a particular location,
67 the Bay of Fundy, eastern Canada.

68

69 The dinoflagellates, *Alexandrium fundyense* is known to produce paralytic shellfish
70 poisoning (PSP) toxins in the Bay of Fundy and neighboring Gulf of Maine. PSP toxins
71 can accumulate in shellfish through filter-feeding, and are potentially fatal to vertebrate
72 consumers (Prakash et al. 1971, Martin and Richard 1996, Hamer et al. 2012). This
73 harmful algal species affects wild fisheries as well as finfish and shellfish aquaculture in
74 the region. *A. fundyense* has been responsible for Atlantic salmon (*Salmo salar*)

75 poisoning and mortalities in the Bay of Fundy (Martin et al. 2008), when concentrations
76 reached 2.0×10^5 cells•L⁻¹ (Burrige et al. 2010). *A. fundyense* was also responsible for
77 Atlantic herring (*Clupea harengus harengus*) mortalities in 1976 and 1979 (White 1977,
78 1980).

79

80 *A. fundyense* is considered to be harmful for vertebrate consumers of shellfish even when
81 cells are present at low densities in natural waters, with counts of 200 cells•L⁻¹ being
82 considered to be the level at which toxicity can be detected in shellfish in the Bay of
83 Fundy (Martin et al. 2010b; J.L. Martin, pers comm). Values of around 500 cells•L⁻¹ can
84 lead to levels of shellfish toxicity above the threshold accepted for human consumption
85 (80 µg STX equiv. 100 g meat), leading to closures of shellfish harvesting areas (Page et
86 al. 2004, J.L. Martin pers. comm.). Many countries throughout the world, including
87 Canada, have extensive programs to monitor toxins in shellfish to comply with domestic
88 and international regulations that ensure safe products for consumers.

89

90 Variables including the timing of the *Alexandrium* spp. blooms (temporal and spatial
91 variations in abundance), and environmental conditions prior to, during, and after these
92 occurrences, are being studied in some areas, to understand the population dynamics of
93 this species. These observations have revealed a complex pattern of seasonal variations,
94 with the species generally beginning to appear in the water column in late spring (May)
95 and subsiding in late summer (July/August) (Martin et al. 2010b). There is strong
96 interannual variability in the timing, intensity, and regional distribution of the cells (Page
97 et al. 2004). During the winter resting period, cysts of *A. fundyense* tend to occur in high

98 concentrations in areas of mud/clay bottoms rather than gravel/rocky bottom sediments.
99 A high abundance of resting cysts in the winter does not correlate with large blooms of *A.*
100 *fundyense* in the summer months (Martin et al., 2014). Many years of observations have
101 shown that *A. fundyense* cells first appear in the water column when the water
102 temperature begins to increase, and the population multiplies exponentially in low-wind
103 and low-light conditions associated with fog (Martin et al. 2014a). The identification of
104 the exact environmental conditions that trigger the occurrences and propagation of *A.*
105 *fundyense* cells continues to be elusive (Townsend et al., 2005, 2014). These complexities
106 have made it difficult to model and predict *A. fundyense* blooms with a view to
107 minimizing risks to seafood consumers and damage to the aquaculture industries.
108
109 It is difficult, if not impossible, to develop a large-scale warning system that relies solely
110 on *in situ* measurements. For instance, automated moorings and buoys, despite measuring
111 water properties with high temporal resolution are not able to capture changes that may
112 occur several kilometers upstream or downstream of their location. This has led to the
113 investigation of the use of satellite remote sensing based on sea-surface temperature to
114 detect blooms of *A. tamarensis* in the Gulf of Maine (e.g., Keafer and Anderson, 1993). In
115 other regions of the world, algorithms have been developed to identify HABs using
116 satellite ocean-colour measurements (Sathyendranath et al. 1997; Subramaniam et al.
117 1999, 2002, Kahru et al. 1997, Babin et al. 2005, Hu et al. 2010, Tomlinson et al. 2004,
118 2009). Growing interest in the detection of HABs has led to the creation of an
119 international program (the IOC-SCOR GEOHAB programme) that co-ordinates and

120 builds on national, regional and international efforts in HAB research within an
121 ecological and oceanographic context.
122

123 In this study we begin with the method of Keafer and Anderson (1993) and consider
124 whether a combination of variables measured by remote sensing could provide
125 information complementary to what we observe from *in situ* measurements. Recently, Mc
126 Gillicuddy et al. (2015) investigated the use of the Medium Resolution Imaging
127 Spectroradiometer (MERIS) ocean colour data to obtain information on *A. fundyense*
128 blooms in the Bay of Fundy. They concluded that satellite-retrieved chlorophyll-a
129 concentration, an index of phytoplankton biomass, could be useful to track the presence
130 of high phytoplankton biomass. Direct observation of the presence of *A. fundyense* at
131 harmful levels using remote sensing remains difficult, especially considering that levels
132 of toxins in shellfish are considered unsafe even at very low cell concentrations (around
133 $500 \text{ cells} \cdot \text{L}^{-1}$), when *A. fundyense* is not the dominant species in the water column.
134 Furthermore, in the Bay of Fundy, the optical signature of the species closely resembles
135 that of other common phytoplankton species, including diatoms and other dinoflagellates
136 (M.-H. Forget, unpublished data).
137

138 We explore the potential to detect *A. fundyense* indirectly, using indicators of the marine
139 ecosystem that are accessible through remote sensing. In particular we exploit the species
140 succession dynamics evidenced by Townsend et al. (2005) in the Gulf of Maine, where *A.*
141 *fundyense* blooms tend to follow the decline of diatom blooms. Since *A. fundyense*
142 appears when the temperatures increase after the winter minimum, we also used sea-

143 surface temperature (SST) as a proxy for *A. fundyense* observation. The focus of the
144 study is on *A. fundyense* cells present in the surface waters - we do not address the issue
145 of overwintering *A. fundyense* resting cysts, which can be responsible for some winter
146 time shellfish toxicity – either through re-suspension of cells due to digging activities,
147 wave movement or other disturbances. We also investigate whether using a threshold of
148 200 *A. fundyense* cells•L⁻¹ is a realistic target for a remote sensing approach using our *in*
149 *situ* dataset to determine the optimum threshold for a warning system.

150

151 **2. Material and Methods**

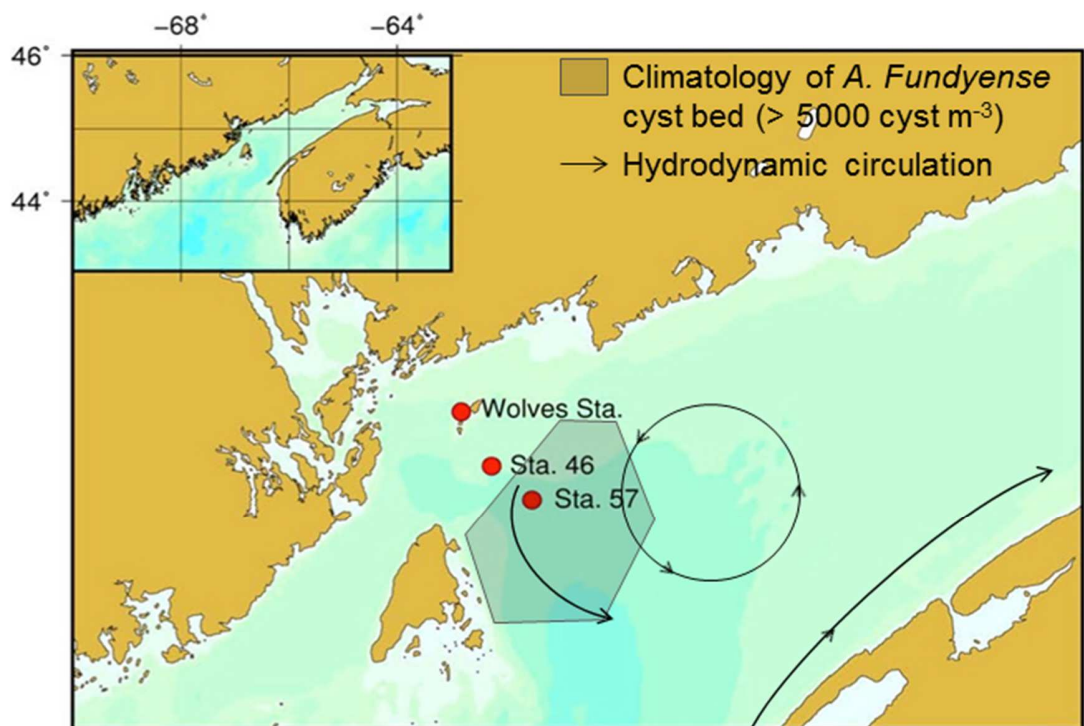
152

153 **2.1 *In situ* data**

154

155 A monitoring program was initiated in 1987 with water samples collected at
156 four/five stations on a monthly basis during the colder months (from November to March
157 each year) and on a weekly basis between April and October to monitor phytoplankton
158 population dynamics, including the toxic algae *A. fundyense* (Martin et al. 2001,2006,
159 2014b), amongst other objectives. From this archive of five stations (See Figure 1, Martin
160 et al. 2014b), we selected data from the most offshore station, i.e., Wolves station (Figure
161 1), between 1998 and 2007 (corresponding to the period of satellite observations), to
162 develop a satellite-based approach to monitor blooms of *A. fundyense*. In 2011, two
163 additional offshore stations were added to the initial sampling plan (stations 46 and 57,
164 Figure 1, Table 1) to create an *in situ* dataset independent of the data used for algorithm
165 development. These three stations were used because of their offshore location, which

166 made them better suited for satellite observations (i.e., reduced contamination of the
167 marine signal by land) than in-shore stations. We limited the original dataset from early
168 May to mid-July to focus our study on the timing of *A. fundyense* blooms. Station Wolves
169 is located 7.5 and 16.5 km from stations 46 and 57 respectively while station 46 and 57
170 are separated by 9.5 km.



171
172 *Figure 1: Sampling stations in the Bay of Fundy, eastern Canada: The Wolves and off*
173 *shore stations 46 and 57.*

174

175

176 Sampling was conducted aboard the Canadian Coast Guard Research Vessel, *Viola M.*

177 *Davidson* and on the Huntsman Marine Science Center vessel *Fundy Spray*.

178 Phytoplankton samples were collected from the water surface by bucket for all three
 179 stations. During the summer months a 10 m vertical plankton haul was made with a 20-
 180 μm mesh net, 0.3 m in diameter. A subsample was preserved with formalin:acetic acid
 181 (1:1 by volume) for plankton identification. Water samples (250 mL) were preserved with
 182 5 mL formalin:acetic acid. Samples were brought back to the laboratory and 50-mL
 183 subsamples were allowed to settle in Zeiss counting chambers for 16 h before
 184 microscopic examination. All phytoplankton of size greater than 5 μm were identified
 185 and enumerated (as $\text{cells}\cdot\text{L}^{-1}$) using a Nikon inverted microscope.

186

187 *Table 1: Station name, station number, location, period of sampling*

Name	N	Longitude	Latitude ($^{\circ}\text{W}$)	Period of sampling
Wolves Islands	16	-66.73	44.97	1998-2011
Off shore 1	46	-66.67	44.89	2011
Off shore 2	57	-66.59	44.84	2011

188

189

190 **2.2 Satellite Data**

191

192 *2.2.1 Satellite datasets for algorithm development*

193 Daily remote sensing reflectance (level 2) data from the Sea-viewing Wide Field-of-view
 194 Sensor (SeaWiFS) were downloaded from the NASA ocean-color website
 195 (<http://oceancolor.gsfc.nasa.gov>). Images over the Bay of Fundy covering the *in situ*
 196 sampling stations were downloaded from April to July between 1998 and 2007.

197 Chlorophyll-a concentration, an index of phytoplankton biomass, was derived using the
 198 OC4 algorithm (O'Reilly et al., 1998). The algorithm developed by Sathyendranath et al.
 199 (2004) was applied to the remote-sensing reflectance to derive, on a pixel-by-pixel basis,
 200 the probability of the occurrence of diatoms, expressed on a scale from 0 to 1 over an
 201 eight-day period of observation. In brief, the algorithm is based on look-up-tables to
 202 derive chlorophyll-a concentration from remote-sensing reflectance for two possible
 203 populations of phytoplankton, one dominated by diatoms and one made of a mix of
 204 phytoplankton. Each of these two phytoplankton populations has different absorption
 205 properties, which were derived by studying the relationships between the composition
 206 and concentration of pigments (i.e., chlorophyll-a, fucoxanthin and chlorophyll-c₃,
 207 Sathyendranath et al, 2004). Using a semi-analytical reflectance algorithm
 208 (Sathyendranath and Platt, 1997, 1998), reflectance ratios 490:670 and 510:555 are
 209 computed for chlorophyll-a ranging from 0.01 to 64 mg m⁻³ for the two possible
 210 populations (see Figure 3 Sathyendranath et al. 2014). On a pixel-per-pixel basis, the two
 211 chlorophyll-a concentrations (i.e., chl-a_{490:670} and chl-a_{510:555}) are computed for each
 212 population (i.e., diatom and mixed) giving a total of four chlorophyll-a concentrations.
 213 The lowest coefficient of variation, CV_{*i*}, where *i* stands for diatom or mixed population,
 214 computed as:

215

$$216 \quad CV_i = \left(\frac{\sigma(\text{chl-a}_{490:670}, \text{chl-a}_{510:555})}{(\text{chl-a}_{490:670}, \text{chl-a}_{510:555})_i} \right), \quad (1)$$

217 provides the population in the pixel. A value of 1 is returned if the population of
 218 phytoplankton is dominated by diatoms (CV_{diatom} < CV_{mixed}) and 0 if this is not the case.

219 Because sediment loads and colored dissolved organic matter would impact the four

220 chlorophyll-a concentrations, and therefore the coefficient of variation (CV), in a similar
221 fashion, we believe that the diatom algorithm remains valid in coastal waters, as attested
222 by the phenology of diatoms which is consistent with species succession recorded in this
223 region (Johnson et al., 2017). Daily satellite passes were averaged into eight-day
224 composite images using the arithmetic mean of all available values for a given pixel
225 during that time period, which yielded a probability of occurrence of diatoms
226 (subsequently expressed in %) for each pixel. The probability of occurrence of diatoms
227 and chlorophyll-a concentration were projected on an equal-area grid with a 1.5 km
228 resolution (2.25 km² per pixel).

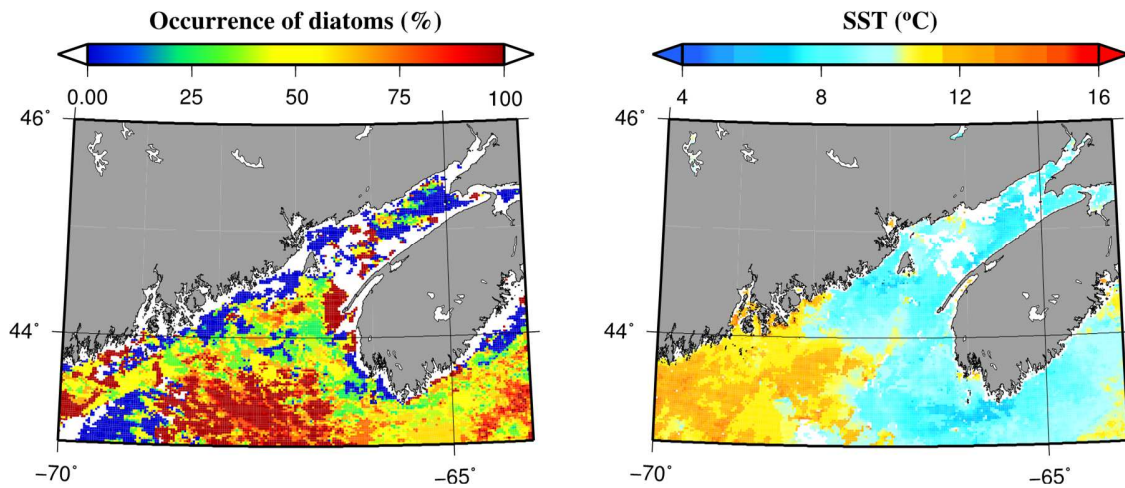
229 Daily Sea Surface Temperature (SST) data from the Advanced Very High Resolution
230 Radiometer (AVHRR) pathfinder version 5.2 (PFV5.2) time series were downloaded
231 from the NASA Jet Propulsion Laboratory archive (<http://podaac.jpl.nasa.gov>) for the
232 same time period and region as the ocean-colour data. The PFV5.2 data are an updated
233 version of the Pathfinder Version 5.0 and 5.1 collections described in Casey et al. (2010).

234

235 Global L3 SST data were averaged over an eight-day period and projected on the 1.5 km
236 grid from the initial 4 km resolution (0.044°). An example of satellite-derived probability
237 of diatom occurrence (PDO) and SST for the Bay of Fundy is shown in Figure 2.

238 For each satellite dataset (i.e., eight-day composite images of SST, diatom occurrence
239 and chlorophyll-a concentration), 5x5 matrices centered on the Wolves station were
240 extracted for the times series. Eight-day composites were selected to reduce the impact of
241 cloud cover while keeping a temporal resolution consistent with the *in situ* sampling. A
242 total of 74 match-ups between satellite data and *in situ* measurements were obtained, over

243 the years 1998 – 2007. Note that the initial *in situ* dataset had 118 samples where the
244 abundance of *A. fundyense* was enumerated, but 44 were not exploitable due to missing
245 information on SST, diatoms or both sets of satellite data because of cloud cover, despite
246 the 8-day binning.



247
248

249 *Figure 2: Composite (24-31 May 2006) image of the Bay of Fundy showing the*
250 *probability of occurrence of diatoms derived from the SeaWiFS sensor and sea-surface*
251 *temperature (SST) derived from the AVHRR sensor for the same period, and same*
252 *location. Occurrence of diatoms is given as a percentage probability (0 – 100) of finding*
253 *diatom-dominated populations in that area during that time interval.*

254

255 2.2.2 Satellite dataset for algorithm validation

256 The algorithm was developed using SeaWiFS data for the years 1998 to 2007. Because of
257 intermittent failure of the sensor from 2007 to 2010, NASA terminated the mission in
258 2010. For the year 2011, data from ESA’s MERIS sensor were used to estimate the
259 occurrence of diatoms (sea-surface temperature was inferred from AVHRR data for the
260 1998-2007 time series). The diatom algorithm was adapted from SeaWiFS to MERIS
261 instead of the Moderate Resolution Imaging Spectroradiometer (MODIS) because it

262 required only minor tuning of the algorithm to account for 5 nm shifts in two of the
263 wavebands (560 and 665 nm) used to discriminate diatoms, whereas no band shifting was
264 required for the other two wavebands (490 and 510 nm). Daily, full-resolution (300 m at
265 nadir) level-2 MERIS data from January to August 2011 over the Bay of Fundy were
266 downloaded from the NASA Ocean Color website (<http://oceancolor.gsfc.nasa.gov>).
267 These data were composited into eight-day images with a resolution of 1.5 km, as was
268 done for the SeaWiFS dataset. Satellite data coincident with *in situ* *A. fundyense* cell
269 counts were extracted at the Wolves, Sta. 57 and Sta. 46 for the year 2011, which yielded
270 a total of 25 data points for validation of the algorithm.

271

272 **2.3 Warning system for possible toxic levels of *A. fundyense***

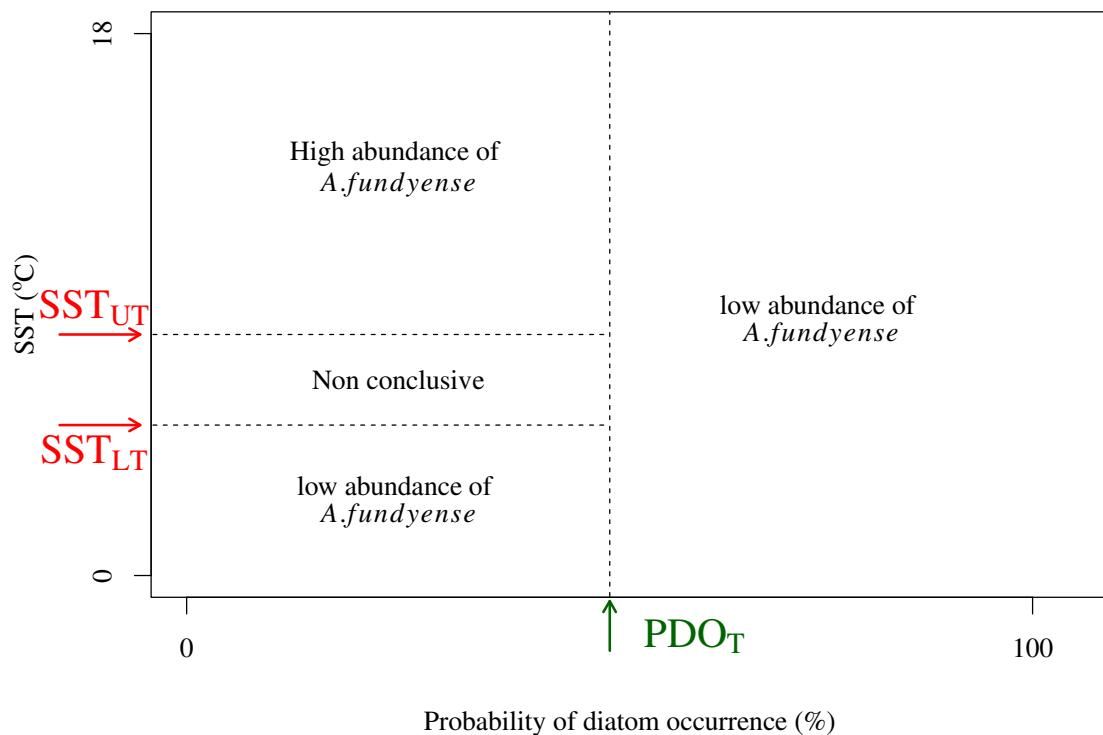
273

274 Given the difficult task of inferring *A. fundyense* cell concentrations using satellite remote
275 sensing information, a simple model that uses three levels of warning (safe = green;
276 inconclusive = orange; harmful = red) was developed based on sea-surface temperature
277 and the probability of diatom occurrence (PDO). In agreement with the information
278 provided by the climatology, the three threshold levels that are used to detect favourable
279 conditions (or not), for the presence of *A. fundyense*, as illustrated in Figure 3 are as
280 follows:

- 281 • PDO above a given threshold, PDO_T , indicates safe conditions (no toxic *A.*
282 *fundyense* cell concentrations):
- 283 • PDO below PDO_T and SST below a lower threshold, SST_{LT} , indicates safe
284 conditions (no toxic *A. fundyense* cell concentrations):

- 285 • SST above an upper threshold, SST_{UT} and PDO below PDO_T indicates likelihood
286 of high concentrations of toxic *A. fundyense* cells
- 287 • PDO below PDO_T and SST between SST_{LT} and SST_{UT} - no conclusive indication
288 of toxic level of *A. fundyense*.

289 In developing the warning system, optimum values have to be found for the thresholds
290 PDO_T , SST_{LT} and SST_{UT} that lead to the best performance of the algorithm (see Figure 3
291 schematic).



292 Probability of diatom occurrence (%)
293 *Figure 3: Schematic of the satellite-based warning system that relies on two SST*
294 *thresholds and one PDO threshold to infer safe, non-conclusive and toxic level of A.*
295 *fundyense.*

296

297 A sensitivity study was carried out to find the optimum thresholds that provided the best
298 performance (i.e., success rate) of the algorithm. Abundance of *A. fundyense* was varied

299 between 100 and 600 cells•L⁻¹ (step of 50 cells•L⁻¹), PDO was varied between 30 and
300 80% (step of 5%) to find the optimum threshold PDO_T, and SST was varied between 4.4
301 and 6° C (step of 0.1° C) to find the lower temperature threshold, SST_{LT}, and the upper
302 SST was varied between 6 and 9° C (step of 0.1° C) to find the upper temperature
303 threshold, SST_{UT}. This led to a total number of 63,767 possible cases. The objective of
304 this sensitivity study was to simultaneously find the lowest *A. fundyense* cell
305 concentration that can be most successfully predicted by proxy using SST and PDO, and
306 the corresponding SST and PDO criteria. For each case of this sensitivity study, a
307 weighted score was assigned according to a comparison of the satellite warning system
308 prediction versus the actual *in situ* measurements of *A. fundyense* abundance as follows:

- 309 • *In situ A. fundyense* abundance is potentially toxic and satellite response is red:
310 1.25 points,
- 311 • *In situ A. fundyense* abundance is not potentially toxic and satellite response is
312 green: 1 point,
- 313 • *In situ A. fundyense* abundance is potentially toxic and satellite response is
314 orange: 0.5 point,
- 315 • *In situ A. fundyense* abundance is not potentially toxic and satellite response is
316 orange: 0.25 point,
- 317 • *In situ A. fundyense* abundance is potentially toxic and satellite response is green
318 (false negative): -1 points,
- 319 • *In situ A. fundyense* is not potentially toxic and satellite response is red (false
320 positive): 0 points.

321 This scoring system was weighted to emphasize the ability to predict potential toxic
322 levels of *A. fundyense* cells; in that respect, agreement between the satellite and *in situ*
323 data for potential toxic levels of *A. fundyense* is weighted at 1.25 points and false
324 negatives are given a negative score (-1).

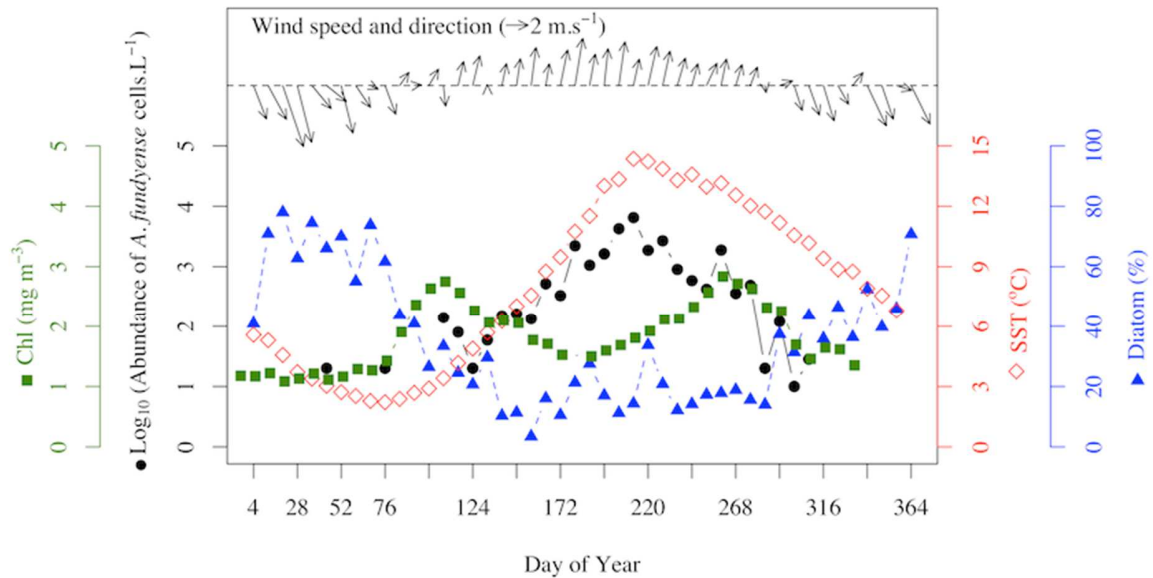
325

326 **3. Results**

327 **3.1 Phenology and spatial variation of *A. fundyense*, diatom occurrence and Sea-** 328 **Surface Temperature**

329 Phytoplankton phenology in the Bay of Fundy derived from satellite data follows
330 the pattern commonly observed at temperate latitudes, with a strong bloom in late
331 March/early April (Vargas et al. 2009, Platt et al. 2009, Racault et al. 2012, Martin et al.
332 1995, 1999, 2001, 2006) with the probability of diatom-dominated populations being
333 consistently high in early Spring (Figure 4). Climatological data of satellite-derived
334 occurrence of diatoms and *in situ* measurements of *A. fundyense* abundance reveals an
335 interesting succession in the development and termination of blooms of these two species.
336 Analysis of the climatological data suggests that the development of *A. fundyense* blooms
337 may be related to the decrease in diatom abundance, as well as the increase in SST and a
338 change in wind patterns. McGillicuddy (2010), studying *A. fundyense* in neighbouring
339 Gulf of Maine, reported similar relationships with temperature and winds. Termination
340 of the *A. fundyense* bloom is not discussed in the present study; however, it often
341 coincides with the onset of the fall diatom bloom when the probability of diatom
342 occurrence increases monotonically to greater than 40% (day 292). Extreme events such
343 as storms and persistent strong winds are also known to end *A. fundyense* blooms. It is

344 noteworthy that a high PDO (~80%) occurs in the winter months when chlorophyll-a
 345 concentration is moderately high (~1.2 mg m⁻³), while the probability of diatom
 346 occurrence at the chlorophyll-a maximum (~ 2.9 mg m⁻³ on day 130) is only about 40%.

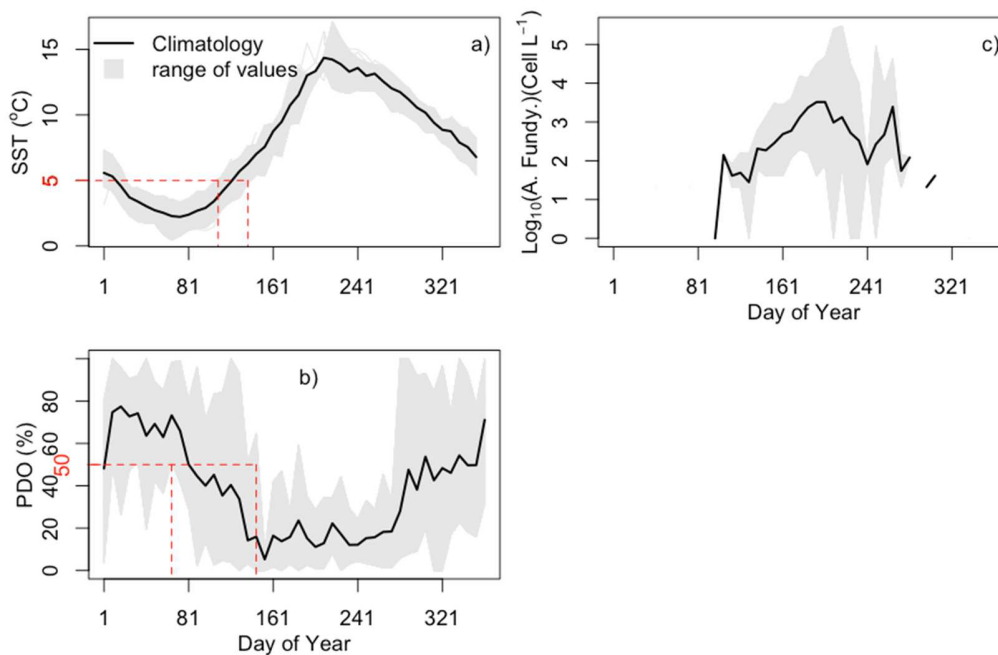


347
 348 *Figure 4: Eight-day climatology (1998-2007) of satellite-derived SST (red diamonds),*
 349 *probability of occurrence of diatoms (blue triangles), chlorophyll-a concentration (green*
 350 *squares) and wind speed and direction, as well as in situ cell abundance of A. fundyense*
 351 *(black Circle) in the Bay of Fundy (Wolves station).*

352

353 The diatom algorithm relies on spectral differences in the remote sensing reflectance and
 354 is independent of the biomass at the first order, whereas the chlorophyll-a algorithm,
 355 based on band-ratios, depends mainly on the magnitude of the remote sensing spectra,

356 and therefore biomass.



357

358 *Figure 5: Eight-day climatology (1998-2007) and range of variation of a) satellite-*
359 *derived SST, b) probability of occurrence of diatom and c) in situ cell abundance of A.*
360 *fundyense at the Wolves station.*

361

362 Sea-surface temperature and probability of occurrence of diatoms show a strong
363 interannual variability (Figure 5 a and b). As an indicator, we have selected the first time
364 that sea-surface temperature is warmer than 5 degrees during the spring, which occurs
365 between early (~ 1st) and late (~ 21st) June, showing a temporal variability of three weeks,
366 in agreement with the high variability observed with the timing of *A. fundyense*. The
367 termination of the phytoplankton diatom spring bloom shows an even wider range of
368 variation than the SST. This is not surprising given the number of environmental factors
369 that can explain shift and successions in phytoplankton population (e.g., nutrient

370 availability, strength of stratification and depth of the mixed layer). As an indicator of the
371 timing of the termination of the diatom dominance, we have recorded the day after which
372 probability of occurrence of diatoms remains below 50% for three successive eight-day
373 composite images. This occurs between the end of March (~ 21st) and end of June (~30th),
374 such that the decline in diatom occurrence is spread over a 12-week period. The earliest
375 initial occurrence of potentially toxic concentrations of *A. fundyense* cells (> 200
376 cells•L⁻¹) was recorded on 13 May 2005 while the latest initial occurrence was recorded
377 on 7 June 2007 at the Wolves station (Figure 5c). This corresponds to a four-week
378 window in the onset of the *A. fundyense* bloom for the period of observation in the study
379 area. The probability of diatom occurrence reached levels of up to 80% in late winter
380 /early spring (day of year 28 to 84) whereas concentrations of *A. fundyense* remain low
381 during the same time period (less than 100 cells•L⁻¹). Following the sharp decrease in the
382 PDO around days 85 to 116, an increase in *A. fundyense* concentrations was observed
383 starting around day-of-year 124 (i.e., beginning of May, 100 cells•L⁻¹) and reaching a
384 maximum in summer, with abundances often greater than 10,000 cells•L⁻¹ (Figure 4).
385 During the sampling period, the onset of the exponential growth phase of *A. fundyense*
386 coincided with an increase in SST, and a change in wind patterns from a southeastward
387 direction to a northeastward direction (Figure 4). Information on the phenology of SST
388 and PDO reveals that the decline of the diatom bloom is a necessary but not sufficient
389 condition for the development of *A. fundyense*. It is also noteworthy that diatom
390 dominance shows a strong spatial variability compared to SST (Figure 2), perhaps in a
391 similar fashion to *A. fundyense*. This pattern is revealed when comparing the properties at
392 the three offshore stations and notably the correlation, or absence of correlation, between

393 SST, POD and *A. fundyense* over the period of sampling between late April (~ 23rd) and
 394 late July in (~20th) 2011 (Table 2).

395

396 *Table 2: Correlation coefficients (r^2) between stations Wolves, 46 and 57 for sea-*
 397 *surface temperature, probability of occurrence of diatom and abundance of *A. fundyense*.*

	SST			POD			<i>A. fundyense</i> abundance		
	Wol.	St. 46	St. 57	Wol.	St. 46	St. 57	Wol.	St. 46	St. 57
Wol.	1			1			1		
St. 46	0.94	1		0.32	1		0.96	1	
St. 57	0.93	0.98	1	0.32	0.54	1	0.42	0.39	1

398

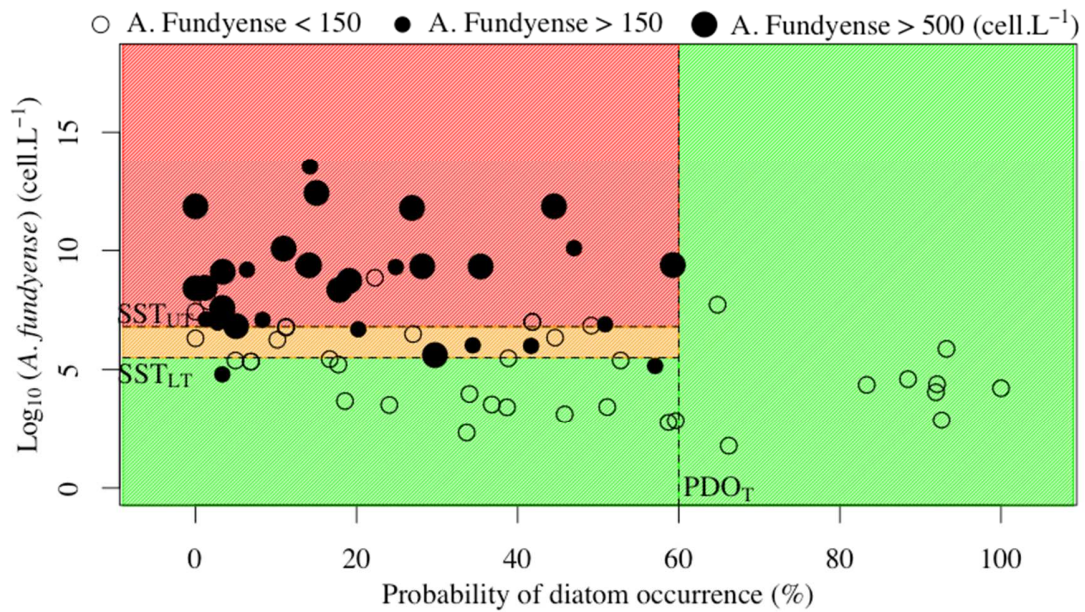
399 Sea-surface temperature shows a high positive correlation coefficient between the three
 400 stations (> 0.93), which is consistent with the rather homogeneous spatial distribution of
 401 SST and is also in agreement with the seasonal and interannual variation of SST (Figure
 402 5), which showed the least variation (e.g., reaching the 8 degree threshold over a 3-week
 403 period between 1998 and 2007 at the Wolves station). The correlation coefficients
 404 between the 3 stations for POD and *A. fundyense* abundance show weaker relationships
 405 ($r^2 < 0.54$) than ones observed for SST, except for *A. fundyense* between stations 46 and
 406 Wolves ($r^2 = 0.96$). The mean *A. fundyense* abundance at stations Wolves, 46 and 57 are
 407 1053(± 1926), 370 (± 803) and 313 (± 439) cell.L⁻¹ respectively and exhibit a decreasing
 408 gradient from the coast towards the center of the Bay of Fundy. The mean SST remains
 409 homogeneous between all three stations: Wolves = 10.4 ± 3.1 °C, station 46 = 10.7 ± 4.4
 410 and station 57 = 10.5 ± 3.3 °C. The POD shows similar means at stations Wolves and 46

411 (44 ± 21% and 47 ± 21 %), which are slightly higher than the mean POD at station 57 (40
412 ± 21%), despite similar average conditions over the period of observation (almost 2
413 months).

414

415 **3.2 SST and PDO thresholds for *A. fundyense* warning system**

416 The weighted scoring system described in the methods section was applied to the
417 development dataset (N=74) for all the possible sets of thresholds (i.e., SST_{LT}, SST_{UT} and
418 PDO_T). This resulted in scores that varied between 25.75 (worse performance) and 55.75
419 (best performance). The best score (55.75) was obtained for a detection level of *A.*
420 *fundyense* counts of 150 cells•L⁻¹ and corresponded to thresholds of 60% for the
421 probability of occurrence of diatoms, 5.5°C for the lower sea-surface temperature
422 threshold and 6.8° for the upper SST threshold (the same score was also obtained for a
423 SST_{LT} of 5.6°C). Figure 6 shows the application of these thresholds together with *A.*
424 *fundyense* cell counts and corresponding SST and PDO measurements for each sample.



425

426 *Figure 6: A. fundyense cell abundance as a function of SST and probability of diatom*
 427 *occurrence using the development dataset. Warning alerts (threshold 1 to 3) are colour-*
 428 *coded from green, to orange to red for low, inconclusive and high risk of toxicity,*
 429 *respectively.*

430

431 The success rate of the algorithm under these criteria is 73% (Table 3), or 54 out of 74
 432 cases. Among these 54 well-identified cases, 28 were classified as toxic levels of *A.*
 433 *fundyense* and 26 were correctly identified as safe levels of *A. fundyense* abundance. Only
 434 3% (2 out of 74 cases) resulted in false negative warnings and 9% in false positive alerts
 435 (7 out of 74 cases). Of the remaining cases, 15% (or 11 out of 74) were not conclusive
 436 (orange warning level), when adding these 11 cases to the proper assessment of *A.*
 437 *fundyense* level, the algorithm reaches a success rate of 88%. When applied to the
 438 validation dataset (N=25), the success rate remained similar to that of the development

439

440 *Table 3: Matchup between satellite and in situ warning levels of A. Fundyense cell*
 441 *concentrations for the development dataset (N=74). The threshold for A. fundyense*
 442 *concentration for satellite detection is 150 cell.L⁻¹.*

		Satellite		
		Toxic	Safe	
<i>In situ</i>	Toxic	28	11	2
	Safe	7	26	
		9% False positive		88% success
				3% False negative

443

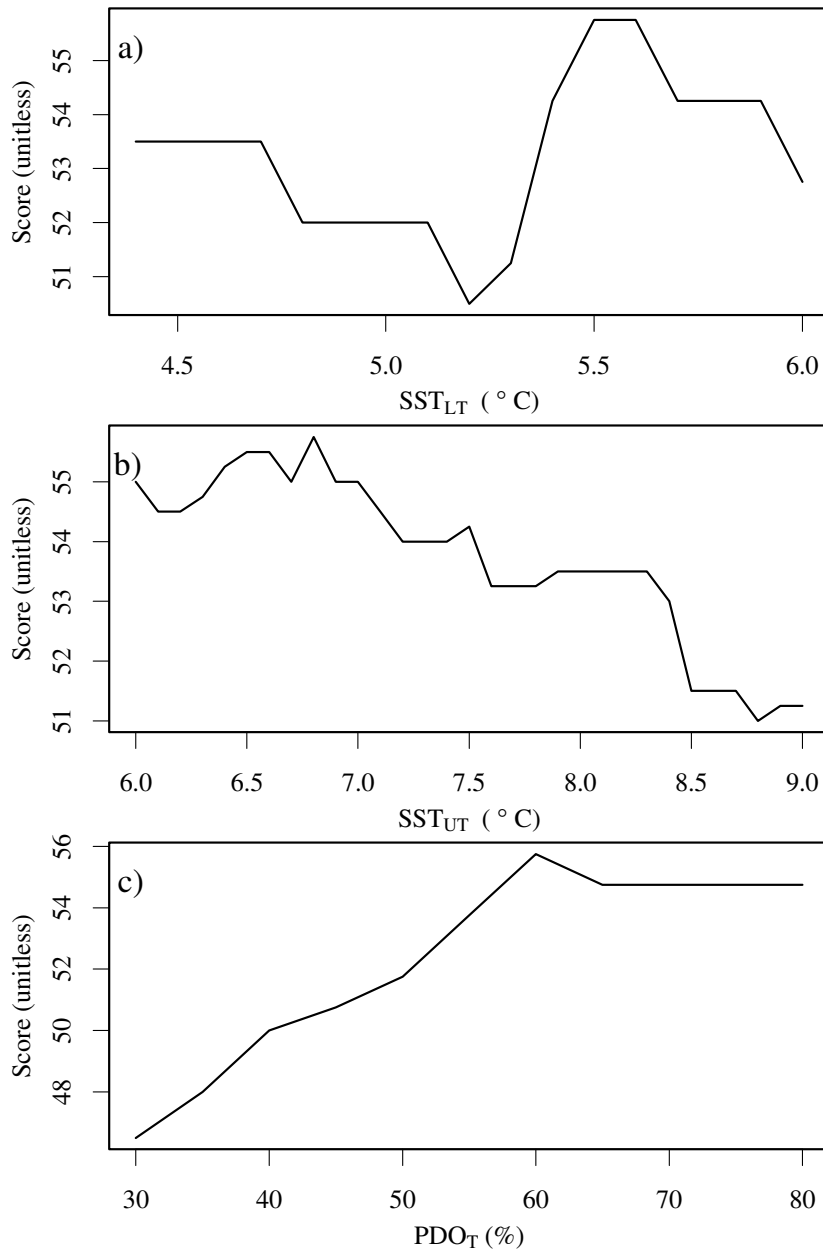
444 *Table 4: Matchup between satellite and in situ warning levels of A. Fundyense cell*
 445 *concentration for the validation dataset (N=25). The threshold for A. fundyense*
 446 *concentration for satellite detection is 150 cell.L⁻¹.*

		Satellite		
		Toxic	Safe	
<i>In situ</i>	Toxic	12	1	4
	Safe	1	7	
		4% False positive		80% success
				16% False negative

447

448 dataset with an overall success rate of 76% (Table 4), which reaches 80% when
449 accounting for the orange level. The percentage of false negative warnings is 16%, false
450 positive warnings and inconclusive cases were both equal to 4%.

451 Variation of the scores as a function of the lower SST threshold shows a continuous
452 decrease between 4.4 and 5.2 °C followed by a sharp increase to reach the maximum
453 score at a temperature of 5.5 or 5.6 °C (Figure 7a). Beyond the SST_{LT} value of 5.6 °C, one
454 observes a monotonic decrease. The score remains fairly high for the upper SST
455 threshold from 6 to 6.8 °C, reaching the maximum value at 6.8 °C and then decreases
456 rapidly as SST increases (Figure 7b). These results demonstrate the narrow ranges of
457 lower and upper temperature thresholds at which the algorithm performs best. For the
458 probability of diatom occurrence threshold (Figure 7c), the score increases from 30 to
459 60% PDO followed by a small decrease, then remains constant past a value of 65%, a
460 function of the training dataset, which contains only few cases with high PDO.



461

462 *Figure 7: Performance score of the warning algorithm as a function of a) lower*
 463 *threshold of sea-surface temperature (SST_{LT}), b) upper threshold of sea-surface*
 464 *temperature (SST_{UT}) and c) threshold of probability of occurrence of diatom (PDO_T).*

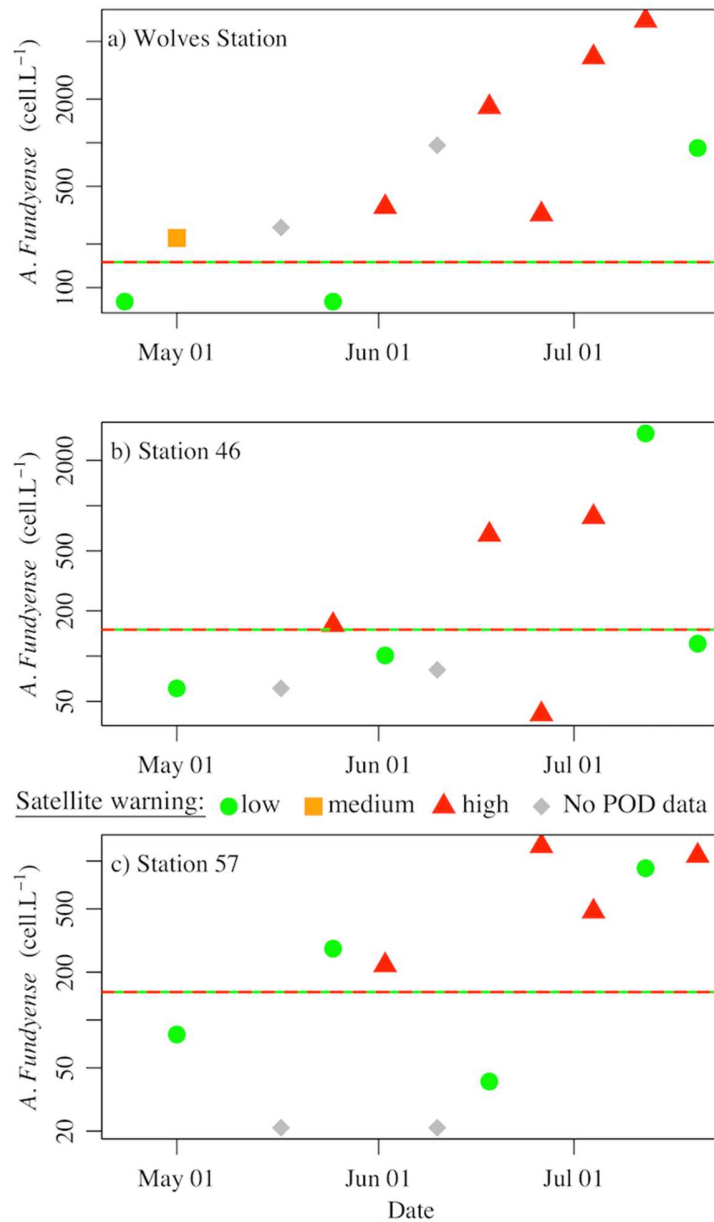
465

466

467 **3.3 Detection of the onset of *A. fundyense* blooms**

468 Even if the algorithm has demonstrated a good overall performance (i.e., ~80% success
469 rate for both the development and validation dataset), a critical assessment of the
470 algorithm lies in its ability to detect the onset of *A. fundyense* exponential growth and
471 variation in timing. Blooms of *A. fundyense* follow a life cycle that can be described in
472 four stages starting with 1) the release of cysts from the bottom of the ocean
473 (excystement) in early spring, 2) a vegetative period, 3) the germination and blooming of
474 *A. fundyense* in late spring and early summer and 4) the sedimentation of newly formed
475 cysts in the fall. Although no direct relationship between the number of cysts and the
476 abundance of cells has been demonstrated (Anderson et al. 2014, Martin et al. 2005,
477 Martin et al. 2014a), the spatial extent of *A. fundyense* cyst beds in the fall/winter drives
478 the spatial distribution of the bloom the following spring. The sediment beds in the
479 central part of the Bay of Fundy (Figure 1) host one of the two major cyst beds in the
480 Gulf of Maine/Bay of Fundy system (Anderson 2014). It has been shown that light and
481 temperature trigger the release of the cysts (Anderson et al. 2005, 2014) into the water
482 column, especially at depths less than 50 m and where transport plays a major role in the
483 distribution of the bloom. Cysts in sediments at depths greater than 100 m tend to have a
484 two-week time lag in germination, compared to those at shallower depths (Vahtera et al.
485 2014), which is in agreement with the timing observed at stations 46 and 57 (Figure 8b-c,
486 respectively), where the first level of abundance greater than 150 cell.L⁻¹ occurs three to
487 four weeks later than at station Wolves (Figure 8a). Station Wolves is located in a
488 relatively shallow part of the Bay of Fundy (60 m) compared to station 46 (111 m), which
489 is located on a strong bathymetric gradient, and station 57 (126 m). Some cysts that are

490 released in the central part of, or close to, the gyre of the Bay of Fundy (stations 46 and
491 57), are leaked at its edges and are carried towards the east (i.e., Gulf of Maine) by the
492 coastal current. In that respect, stations 46 and 57 are located at the edge of the gyre such
493 that the cysts in that area are subject to lateral transport. Our algorithm uses a pixel-based
494 approach that relies on water mass properties to model favourable conditions for *A.*
495 *fundyense* growth. It does not identify the initiation of the bloom per se but rather an
496 abundance of cells for given environmental conditions. The chronological mapping of the
497 warning level in late spring early summer is consistent with known hydrodynamic
498 patterns and bathymetry of the Bay of Fundy, however, it does not provide information
499 on transport and germination of the cells, which are subject to complex, and not fully
500 understood, forcing. Our model rather relies on identification of water masses. Despite
501 this, the algorithm is able to detect the first toxic levels of *A. fundyense* at all stations and
502 provide information on temporal variation. At the Wolves station (Figure 8a), the first
503 occurrence of *A. fundyense* cell concentrations over $150 \text{ cells} \cdot \text{L}^{-1}$ occurs in early May,
504 and is correctly identified as an orange warning by the satellite-based algorithm. The
505 algorithm also records the decrease in *A. fundyense* abundance in late May in agreement
506 with the *in situ* measurements. Again, the algorithm detects the increase in the toxic algae
507 the following week (red level the first week of June) and remains at the red level from
508 early June to mid-July as *A. fundyense* abundance is greater than the $150 \text{ cell} \cdot \text{L}^{-1}$
509 threshold. The satellite warning system is in agreement with *in situ* measurements. In late
510 July, conditions were identified as safe (green) for an abundance of $320 \text{ cells} \cdot \text{L}^{-1}$. In that
511 instance, we observed a sharp decrease in *A. fundyense* abundance, but it was not below
512 the safe level.



514

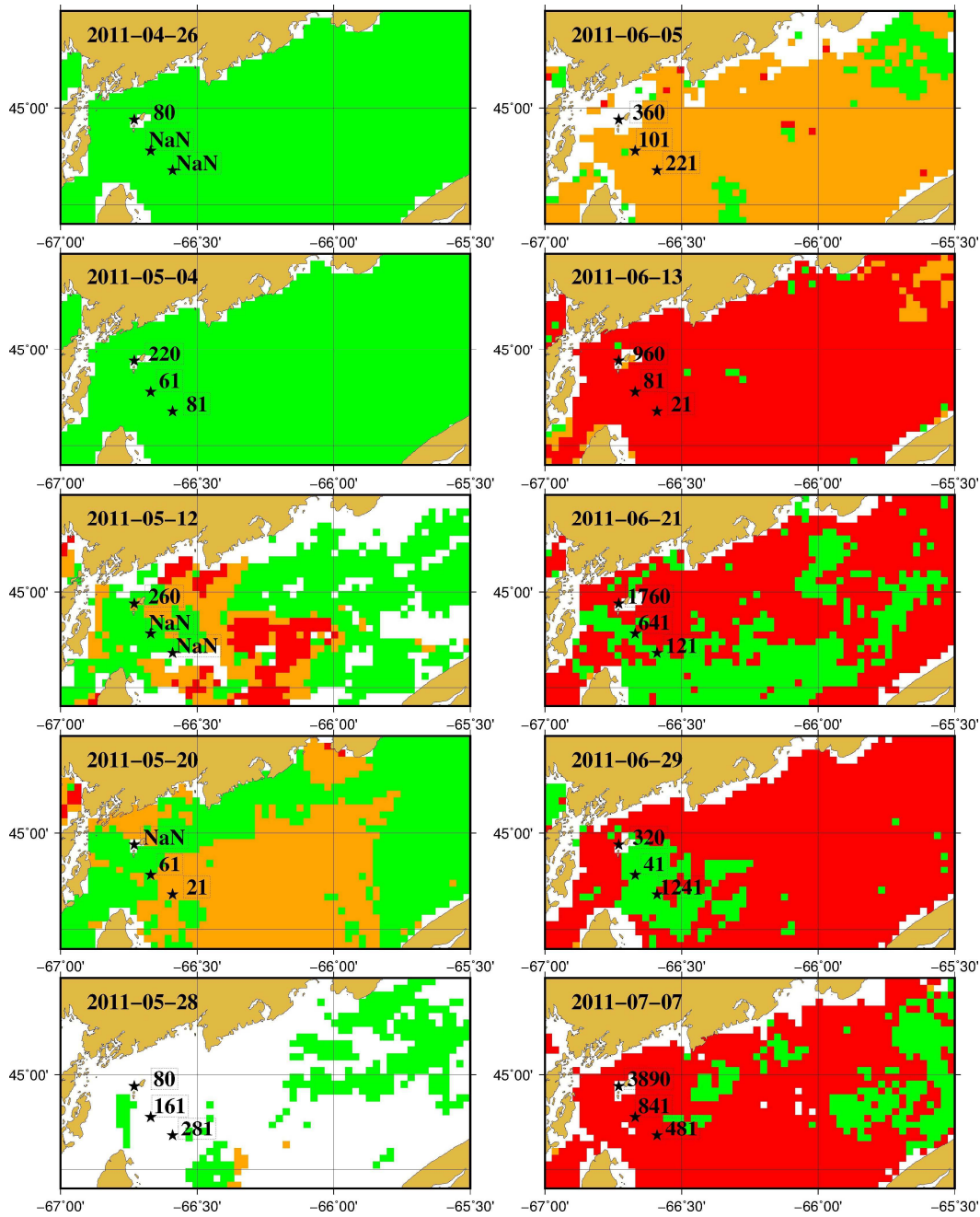
515 *Figure 8: A. fundyense* cell abundance as a function of time at station Wolves (a), station
 516 57 (b) and station 46 (c) for the year 2011. Solid circles are color-coded as a function of
 517 satellite warning level, i.e., green, orange and red for low, inconclusive and high risk of
 518 toxic level of *A. fundyense* cell abundance respectively.

519 Stations Wolves and 46 show very similar temporal variation in *A. fundyense* abundance
520 ($r^2 = 0.96$, Table 2) and the algorithm provides a similar response, recording the first
521 increase in *A. fundyense* at toxic level (May 25th), followed by a decrease below the toxic
522 level (green level, June 2nd) and another increase (June 18th). However, the warning
523 system shows a false positive on the 25th of June. In July, the algorithm is in agreement
524 with the *in situ* measurements, except for a false negative occurring for high abundance
525 of *A. fundyense* ($\sim 3000 \text{ cell.L}^{-1}$). At station 57, the warning system records the first high
526 level of *A. fundyense* with a one week lag, i.e., false negative on the 25th of May.
527 However, the *A. fundyense* abundance is 281 cell.L^{-1} , which is well below the 500 cell.L^{-1}
528 threshold when shellfish are considered unsafe for human consumption. Similarly to
529 stations Wolves and 46, the algorithm detects the sudden decrease in abundance of *A.*
530 *fundyense* (mid-July) to below the toxic level.

531 **3.4 Spatial distribution of *A. fundyense* bloom**

532 We selected the year 2011 to derive information on the development and spatial
533 distribution of *A. fundyense* blooms in the Bay of Fundy (Figure 9) from the 26th of April
534 to the 7th of July (see supplementary material for years 1998 to 2007). The first two
535 weeks of observation show low levels of *A. fundyense*, in agreement with the *in situ*
536 measurements except for a slight elevation of *A. fundyense* abundance (220 cell.L^{-1}) at
537 the Wolves station the last week of April. The first possible toxic level of *A. fundyense*
538 detected by satellite observations occurred mid-May in the central part of the Bay of
539 Fundy (orange/red) in addition to a small area flagged as possible high abundance of *A.*
540 *fundyense* ($> 150 \text{ cells}\cdot\text{L}^{-1}$, red) close to the shore. This large patch of potential *A.*
541 *fundyense* cells with abundance greater than $150 \text{ cells}\cdot\text{L}^{-1}$ spreads during the second half

542 of May. However, the lack of valid pixels in the last week of May prevents comparisons
543 with *in situ* measurements, which show an increase from the previous week with values
544 over the threshold of 150 cells•L⁻¹ at the offshore stations (i.e., 46 and 57). By early to
545 mid- June, in agreement with *in situ* measurements at all stations, the entire region of
546 interest is categorized as orange and red levels of *A. fundyense* abundance, except for two
547 small areas in the northeast and southwest. By the end of June, the satellite observations
548 show the patchy nature of *A. fundyense* bloom, with both low and high levels of warning
549 juxtaposed. Again, the satellite warning system agrees with *in situ* observations. Late
550 June, most of the region is classified as possible high levels of *A. fundyense* abundance
551 except for the central part. It is remarkable that the *in situ* measurements are in agreement
552 with the satellite warning, with stations Wolves and 57 noted as red levels with
553 abundance of *A. fundyense* of 320 and 1241 cell. L⁻¹ respectively, whereas station 46 (41
554 cell. L⁻¹) is located in a region of low abundance of the toxic algae. Finally, for the first
555 week of July, the number of pixels classified as red decreases again, notably from the
556 northeast part of the region of interest. The development of *A. fundyense* in 2011 is
557 similar to observations from previous years (Supplementary material), with a bloom that
558 usually begins in the central part of the Bay of Fundy and spreads towards the coastal
559 areas with high interannual variability in the spatial distribution of the bloom.



560

561 *Figure 9: Eight-day composite image of A. fundyense warning system for the entire Bay*
 562 *of Fundy from the 22 April to 7 July 2011. The color-coding represents low (green ≤ 150*
 563 *cells $\cdot L^{-1}$), medium (orange, inconclusive information on A. fundyense toxicity level) and*
 564 *high (>150 cells $\cdot L^{-1}$) A. fundyense cell abundance. Numbers in boxes indicate the cell*
 565 *abundance of A. fundyense at the Wolves station (black solid star).*

566

567 **4. Discussion and conclusion**

568 Our approach to detect *A. fundyense* blooms relies on the theory of habitat suitability that
569 is extensively used in ecosystem management. One of the main assumptions of this
570 ecological approach is that there is no need to directly detect the organism of interest but
571 rather inform on favorable environmental conditions. This type of approach has been
572 used for a wide range of organisms, ranging from whales in the pelagic environment to
573 habitat mapping in the near-shore. Previous studies have also demonstrated that habitat
574 modeling was useful to derive information on harmful algal blooms, such as the
575 production of domoic acid off the coast of California in the United States of America
576 (Anderson et al., 2016), the detection of the harmful algae *K. mikimotoi* in Ireland using
577 satellite-derived chlorophyll concentration and sea-surface temperature (Raines et al.
578 2010) and forecasting the risk of harmful algal blooms on the Atlantic coast of Europe
579 using satellite remote sensing and other information associated with marine conditions
580 (Davidson et al. 2016).

581 *A. fundyense* cells produce toxins that causes paralytic shellfish poisoning (PSP toxins)
582 and can harm humans that consume shellfish that have accumulated PSP toxins at levels
583 equal or higher than 80 µg toxin per 100 gram of bivalve shellfish edible tissue. It is
584 commonly agreed that 200 cells•L⁻¹ corresponds to the threshold above which toxicity
585 will be detected in shellfish from the Bay of Fundy. Such a low number of cells at which
586 *A. fundyense* cells can result in detectable levels of toxins in shellfish, (compared to an
587 average abundance of phytoplankton of 10³ to 10⁶ cell per liter), as well as an optical
588 signature similar to other phytoplankton species, makes it impossible to directly detect
589 abundance of *A. fundyense* with confidence. Here, we have chosen to use a warning

590 system that can indicate possible high levels of *A. fundyense* abundance in the spring and
591 early summer, a critical time when the rapid increase in *A. fundyense* abundance
592 represents a cause for concern. The warning system uses information on satellite-sea
593 surface temperature and probability of diatom occurrence to infer the possible levels of
594 toxic *A. fundyense* blooms. Rather than attempting to provide a number of cells, we have
595 chosen an approach that will rely on three different levels of warning, for which the
596 probability of occurrence of *A. fundyense* increases from low risks to high risks.

597

598 Our development dataset of *A. fundyense* cell counts, SST and PDO was used to refine
599 PDO and SST thresholds, and estimate the “most detectable” level of *A. fundyense* cell
600 concentrations using a scoring system that favours the detection of high concentrations of
601 *A. fundyense* cells using satellite-retrieved proxies, and penalises the detection of false
602 negative responses (i.e., toxic levels of *A. fundyense* at which shellfish have detectable
603 levels of toxins but no warning by the satellite system). A sensitivity study identified the
604 best set of criteria to infer potentially toxic concentrations of *A. fundyense* cells: our
605 algorithm performed best at $150 \text{ cells} \cdot \text{L}^{-1}$ rather than the recommended concentration of
606 $200 \text{ cells} \cdot \text{L}^{-1}$, which also contributes toward a precautionary approach (information on
607 sea-surface temperature as well as probability of occurrence of diatoms contributes to the
608 flagging of potential toxic levels of *A. fundyense* cells). The PDO_T criteria ($> 60\%$) is
609 more indicative of a safe level of *A. fundyense* (6 out of 8 possible cases) whereas the
610 SST_{UT} threshold ($> 6.8^\circ\text{C}$) appeared to be a better indicator of high concentrations of *A.*
611 *fundyense* (16 out of 18 possible cases). Note that the thresholds in SST and PDO seem to
612 be sensitive to any small variations (Figure 7) such that the performance of the algorithm

613 can rapidly degrade if, for instance, the lower SST threshold changes by half a degree
614 Celsius. Overall, the algorithm was successful in detecting the timing of *A. fundyense*
615 exponential growth phase apart from the offshore station 46. The poor performance of the
616 algorithm at station 46 is explained by high sea-surface temperature (above 11°C and up
617 to 19°C) associated with a low probability of occurrence of diatoms (between 0 and 53%
618 with a mean of 28%) whereas stations 57 and Wolves show levels of diatoms higher or
619 equal to 60% in many instances with means of 40 and 43% respectively. However, the
620 algorithm tends to produce false negatives, which is consistent with the principle of the
621 precautionary approach. The results at station 46 suggest that the algorithm should be
622 adapted for the central waters of the Bay of Fundy where diatom abundance might be
623 lower than on the coast. This next step could be achieved with a larger dataset collected
624 in the central part of the Bay of Fundy spanning a longer time period than the dataset
625 used in this study.

626

627 The spatial development of *A. fundyense* blooms is in agreement with other studies in the
628 area (see Townsend et al., 2001, 2005) as well as the hydrodynamic circulation of the
629 Bay of Fundy (Aretxatabatela et al., 2008, 2014), including the transport and
630 sedimentation of cysts, despite an absence of relationship between cysts and cell
631 abundance of *A. fundyense* (Martin et al. 2014). As was found in the Aretxatabatela et al.
632 studies (2008,2014), the first toxic level of *A. fundyense* occurs in the central and eastern
633 part of the Bay of Fundy, following input of cold, nutrient-rich waters from the Scotian
634 Shelf and contributing to the eastern Maine coastal current. These waters enter the central
635 part of the Bay of Fundy (i.e. the gyre) and spread toward the southwestern regions. Our

636 analysis of the satellite time series of occurrence of toxic levels of *A. fundyense*
637 abundance also reveals the very patchy nature of *A. fundyense* abundance. The ability of
638 the algorithm to detect harmful concentrations of *A. fundyense* constitutes a valuable
639 synoptic complement to *in situ* measurements. Operationally, its application can provide
640 a broad view of the entire basin allowing managers to focus on areas of concern that may
641 not necessarily be included under a monitoring program. This algorithm also provides the
642 ability to detect the first occurrence of high abundance of *A. fundyense* in the central part
643 of the Bay of Fundy.

644

645 A limitation of the algorithm is that it does not account for uncertainties in both *in situ*
646 and satellite measurements. Whereas this might not be an issue in extreme cases (high
647 abundance of *A. fundyense*, low or high SST and high PDO), this might decrease the
648 ability of the algorithm to properly identify a given level of warning. For instance,
649 abundance of *A. fundyense* of 121 cells•L⁻¹ occurred on 22 June 2011, when satellite
650 ocean-colour information indicated a level of occurrence of diatoms of 58.3% and
651 temperature of 16.6 °C. The PDO is very close (less than 2%) to the threshold between
652 safe level of *A. fundyense* abundance (i.e. 60%) and the cell count is close to the detection
653 threshold of 150 cells•L⁻¹, such that the difference between safe and toxic concentration
654 of *A. fundyense* cells is very slim. Similar situations also occur on 13 May 2005 where
655 both SST (5.2 °C) and PDO (57%) are close to the thresholds SST₁ and PDO₁
656 respectively, and on 7 July 2007 when PDO (59%) is close to the safe threshold. .

657

658

659 There is a continued and growing commitment by the international community to monitor
660 HABs due to their socio-economic impact on human activities (e.g., fisheries, tourism,
661 human health). Numerous studies have led to regional approaches, which combine *in situ*
662 and remotely sensed measurements of several parameters (Cannizzaro et al. 2008, Hu et
663 al. 2010, Tomlinson et al. 2009, Carvalho et al. 2010, 2011). Here, we developed a
664 monitoring system for *A. fundyense* in the Bay of Fundy that relies only on satellite
665 remote sensing data. The criteria used to delineate the level of alert for possible presence
666 of *A. fundyense* were defined using SST and occurrence of diatoms. The algorithm
667 showed consistent performance using both the development as well as test datasets, and
668 was in agreement with *in situ* counts of *A. fundyense* in two out of three stations. The
669 algorithm has the tendency to produce false positives which, given the possible impact of
670 *A. fundyense* and resulting shellfish toxicity on human consumers, favors the
671 precautionary approach.

672

673 In early spring, levels of *A. fundyense* are very low to zero, whereas in summer, they are
674 usually well above the minimum threshold of toxicity for shellfish consumption. Satellite
675 observations tend to clearly identify these two periods. The critical time is the onset of
676 the bloom, which is very difficult to predict using *in situ* measurements of *A. fundyense*
677 abundance due to its high spatial and temporal variability. In this respect, the use of
678 satellite remote sensing proxies (SST and probability of occurrence of diatoms) appears
679 as an emerging tool to map the development of *A. fundyense* in time and space. A
680 limitation of the satellite method is the inability to observe the surface of the ocean under
681 cloudy conditions. This limitation can be overcome for SST measurements by using data

682 from the Group for High Resolution Sea Surface Temperature (GHRSSST), which
683 combines data from multiple sensors as well as *in situ* data to provide quality-controlled
684 SST for operational applications. The rapid development of the bloom would also require
685 a higher temporal observation window than the eight-day composite used in this study.
686 The consistency between the two dataset (AVHRR/SeaWiFS (1998-2007) and
687 MODIS/MERIS (2011)) demonstrates the robustness of the algorithm and its potential for
688 recent and future sensors such as the Sea and Land Surface Temperature Radiometer
689 (SLSTR) and Ocean and Land Colour Imager (OLCI) on board the Sentinel-3A platform
690 launched by the European Space Agency (ESA) in February 2016. ESA is planning to
691 launch a second sensor (Sentinel-3B) in the coming year that would help to provide the
692 high temporal resolution required for early detection of *A. fundyense* blooms. Our study
693 also reveals the need for local information on *A. fundyense* to be coupled with satellite
694 observations to extrapolate measurements to the entire Bay of Fundy. Ideally, *in situ*
695 measurements, model simulation and satellite observations should be integrated in a
696 comprehensive observational system that would allow local and regional observation and
697 prediction of *A. fundyense* abundance and growth in the Gulf of Maine and Bay of Fundy
698 regions.

699

700 **Acknowledgement:** We thank the Northeastern Regional Association of Coastal and
701 Ocean Observing Systems (NERACOOS) and the Canadian Space Agency (GRIP
702 program) for funding. The SST data were provided by GHRSSST and the US National
703 Oceanographic Data Center. This project was supported in part by a grant from the
704 NOAA Climate Data Record (CDR) Program for satellites. We also thank the Ocean

705 Biology Processing Group (Code 614.2) at the GSFC, Greenbelt, MD 20771, for the
706 production and distribution of the ocean color data. We thank the Captains and crews of
707 the CCG *Viola M. Davidson* and *Fundy Spray*. M.M. LeGresley helped with sampling,
708 sample preparation and analysis. Finally, we thank the remote sensing group at the
709 Bedford Institute of Oceanographic for support and the two anonymous reviewers for
710 their constructive comments, which significantly improved the initial manuscript.

711

712 **References:**

713

714 Anderson CR, Kudela RM, Kahru M, Chao Y, Rosenfeld LK, Bahr FL, Anderson DM,
715 Norris TA (2016) Initial skill assessment of the California-Harmful Algal Risk Mapping
716 (C-HARM) system. *Harmful Algae* 59:1-18.

717

718 Anderson DM, Townsend DW, McGillicuddy Jr DJ, and Turner JT (2005) The ecology
719 and oceanography of toxic *Alexandrium fundyense* blooms in the Gulf of Maine. *Deep-*
720 *Sea Res II* 52:19-21

721

722 Anderson DM, Keafer BA, Kleindinst JL, McGillicuddy DJ, Martin JL, Norton K,
723 Pilskaln CH, Smith JL. (2014) *Alexandrium fundyense* cysts in the Gulf of Maine: long-
724 term time series of abundance and distribution, and linkages to past and future blooms.
725 *Deep-Sea Res II*, 103:6–26.

726

727 Aretxabaleta, AL, McGillicuddy Jr. DJ, Smith KW and Lynch DR (2008), Model
728 simulations of the Bay of Fundy Gyre: 1. Climatological results, J. Geophys. Res., 113,
729 C10027, doi:10.1029/2007JC004480.
730

731 Aretxabaleta AL, Butman B, Signell RP, Dalyander PS, Sherwood CR, Sheremet VA and
732 McGillicuddy, D. J. (2014). Near-bottom circulation and dispersion of sediment
733 containing *Alexandrium fundyense* cysts in the Gulf of Maine during 2010–2011. *Deep-*
734 *Sea Research. Part II, Topical Studies in Oceanography*, 103, 96–111.
735 <http://doi.org/10.1016/j.dsr2.2013.11.003>
736

737 Babin M, Cullen JJ, Roesler CS, Donaghay PL, Doucette GJ, Kahru M, Lewis
738 MR, Scholin CA, Sieracki ME and Sosik HM (2005) New approaches and technologies
739 for observing harmful algal blooms, *Oceanogr* 18 :210–227
740

741 Burrige LE, Martin JL, Lyons MC, and LeGresley MM (2010) Lethality of microalgae
742 to farmed Atlantic salmon (*Salmo salar*). *Aquaculture* 308:101-105
743

744 Cannizzaro JP, Carder KL, Chen FR, Heil CA, Vargo GA (2008) A novel technique for
745 detection of the toxic dinoflagellate, *Karenia brevis*, in the Gulf of Mexico from remotely
746 sensed ocean color data. *Cont Shelf Res* 28:137–158
747

748 Carvalho GA, Minnett PJ, Fleming LE, Banzon VF and Baringer W (2010) Satellite
749 remote sensing of harmful algal blooms: A new multi-algorithm method for detecting the
750 Florida Red Tide (*Karenia brevis*). *Harmful Algae* 9(5):440-448.
751

752 Carvalho GA, Minnett PJ, Banzon VF, Baringer W, Heil CA (2011) Long-term
753 evaluation of three satellite ocean color algorithms for identifying harmful algal blooms
754 (*Karenia brevis*) along the west coast of Florida: A matchup assessment. *Remote Sens*
755 *Environ* 115(1):1-18.
756

757 Casey KS, Brandon TB, Cornillon P and Evans R (2010) The Past, Present and Future of
758 the AVHRR Pathfinder SST Program, in *Oceanography from Space: Revisited*, eds. V.
759 Barale, J.F.R. Gower, and L. Alberotanza. Springer
760

761 Davidson K, Anderson DM, Mateus M, Reguera B, Silke J, Sourisseau M and Maguire J.
762 (2016) Forecasting the risk of harmful algal blooms preface. *Harmful Algae* 53: 1-7
763

764 Hamer A, Martin JL, Robinson S, Page F, Hill B, Powell F and Justason A (2012)
765 Spatial and temporal trends in paralytic shellfish poisoning levels in the soft shell clam,
766 *Mya arenaria*, along the southwestern coast of New Brunswick in the Bay of Fundy. *Can*
767 *Tech Rep Fish Aquat Sci*, 2982: 97p
768

769 Hartigan JA and Wong MA (1979) A K-means clustering algorithm. *Appl Stat* 28:100–
770 108

771

772 Hu C, Cannizzaro J, Carder KL, Muller-Karger FE, and Hardy R (2010) Remote
773 detection of *Trichodesmium* blooms in optically complex coastal waters: Examples with
774 MODIS full-spectral data. *Remote Sens Environ* 114:2048-2058

775

776 Johnson C, Devred E, Casault B, Head E, and Spry J (2017) Optical, Chemical, and
777 Biological Oceanographic Conditions on the Scotian Shelf and in the Eastern Gulf of
778 Maine in 2015. DFO Can Sci Advis Sec Res Doc 2017/012. v + 53 p

779

780 Kahru M (1999) Monitoring algal blooms: new techniques for detecting large-scale
781 environmental change, *Photosynthet* 36(1-2), 50

782

783 Keafer, BA, and Anderson DM (1993) Use of remotely-sensed sea surface temperatures
784 in studies of *Alexandrium tamarense* bloom dynamics. In: *Toxic Phytoplankton Blooms*
785 *in the Sea*, Elsevier, Amsterdam (Netherlands), *Dev. Mar. Biol.*, vol 3:763-768

786

787 Martin, JL, Wildish DJ, LeGresley MM and Ringuette MM (1995) Phytoplankton
788 monitoring in the southwestern Bay of Fundy during 1990-1992. *Can Manuscri Rep.*
789 *Fish. Aquat. Sci.* 2277: 154 p

790

791 Martin JL and Richard D (1996) Shellfish toxicity from the Bay of Fundy, eastern
792 Canada: 50 years in retrospect. In: Yasumoto T, Oshima Y, Fukuyo Y (eds) *Harmful and*

793 toxic algal blooms. Intergovernmental Oceanographic Commission UNESCO, Paris, p 3–
794 6
795
796 Martin JL, LeGresley MM, Strain PM and Clement P (1999) Phytoplankton monitoring
797 in the southwest Bay of Fundy during 1993-96. Can Tech Rep Fish Aquat Sci 2265: 132p
798
799 Martin JL, LeGresley MM, Strain PM (2001) Phytoplankton monitoring in the western
800 isles region of the Bay of Fundy during 1997-98. Can Tech Rep Fish Aquat Sci 2349: 85
801 p
802
803 Martin JL, LeGresley MM and Strain PM (2006) Plankton monitoring in the western isles
804 region of the Bay of Fundy during 1999-2000. Can Tech Rep Fish Aquat Sci 2629. iv +
805 88 p
806
807 Martin JL, LeGresley MM, Hanke A, and Page FH (2008) *Alexandrium fundyense* - red
808 tides, PSP shellfish toxicity, salmon mortalities and human illnesses in 2003-04 – before
809 and after. *In*: Moestrup et al. (Eds.). Proceedings of the 12th International Conference on
810 Harmful Algae. International Society for the Study of Harmful Algae and
811 Intergovernmental Oceanographic Commission of UNESCO, 2008. Copenhagen. 206-
812 208
813 Martin, JL, Hastey CD, LeGresley MM and Page FH (2010a) Temporal and spatial
814 characteristics of the diatom *Leptocylindrus minimus* in the Western Isles region of the
815 Bay of Fundy. Can. Tech. Rep. Fish. Aquat. Sci.2903: iii+25 p.

816

817 Martin JL, Page FH, LeGresley MM and White J (2010b). Twenty years – *Alexandrium*
818 *fundyense* bloom dynamics in relation to total phytoplankton and shellfish toxicity in the
819 Bay of Fundy. In: Harmful Algae 2008, Proceedings of the 13th International Conference
820 on Harmful Algae, 3-7 November 2008, Hong Kong, China. Editors K-C Ho, M.J. Zhou,
821 and Y.Z. Qi. Environmental Publication House, Hong Kong. p. 53-56.

822

823 Martin JL, LeGresley MM and Hank AR (2014a) Thirty year – *Alexandrium fundyense*
824 cyst, bloom dynamics and shellfish toxicity in the Bay of Fundy, eastern Canada, Deep
825 Sea Res. II, 103:27-39, doi:10.1016/j.dsr2.2013.08.004

826

827 Martin, J.L., M.M. LeGresley, and M.E. Gidney (2014b) Phytoplankton monitoring in the
828 Western Isles region of the Bay of Fundy during 2007-2013. Can Tech Rep Fish Aquat
829 Sci 31XX: v + 262 p.

830

831 McGillicuddy DJ, Townsend DW, He R, Keafer BA, Kleindinst JL, Li Y,
832 Manning JP, Mountain DG, Thomas MA, and Anderson DM (2011) Suppression of the
833 2010 *Alexandrium fundyense* bloom by changes in physical, biological, and chemical
834 properties of the Gulf of Maine, Limnol. Oceanogr., 56(6) :2411–2426,
835 doi:10.4319/lo.2011.56.6.2411

836

837 Page FH, Martin JL, Hanke A, and LeGresley MM (2004) The relationship of
838 *Alexandrium fundyense* to the temporal and spatial pattern in phytoplankton community

839 structure within the Bay of Fundy, eastern Canada. In K.A. Steidinger, J.H. Landsberg,
840 C.R. Thomas and G.A. Vargo (Eds.) Harmful Algae 2002 Florida Fish and Wildlife
841 Conservation Commission, Florida Institute of Oceanography, and Intergovernmental
842 Oceanographic Commission of UNESCO, St. Petersburg, Florida, USA. pp. 92-94
843

844 Prakash A, Medcof JC and Tennant AD (1971) Paralytic shellfish poisoning in eastern
845 Canada. Bull. Fish. Res. Board Can. 177:87 p
846

847 Platt, T, White III GN, Zhai L, Sathyendranath S and Roy S (2009) The phenology of
848 phytoplankton blooms: Ecosystem indicators from remote sensing. Ecol. Modeling,
849 220(21):3057-3069
850

851 Racault, MF, Le Quéré C, Buitenhuis E, Sathyendranath S and Platt T (2012)
852 Phytoplankton phenology in the global ocean, Ecological Indicators 14:152–
853 163, doi: 10.1016/j.ecolind.2011.07.010
854

855 Raine R, McDermot G, Silke J, Lyons K, Nolan G, and Cusack, C (2010) A simple short
856 range model for the prediction of harmful algal events in the bays of southwestern
857 Ireland. J. Mar. Syst. 83: 150-157
858

859 Sathyendranath, S, Subba Rao, DV, Chen, Z, Stuart, V, Platt, T, Bugden, GL, Jones, W,
860 Vass, P (1997) Aircraft remote sensing of toxic phytoplankton blooms: a case study from
861 Cardigan River, Prince Edward Island. *Can. J. Remote Sens.* 23: 15-23.

862

863 Sathyendranath S, Watts L, Devred E, Platt, T, Caverhill C and Maass H (2004)

864 Discrimination of diatoms from other phytoplankton using ocean-colour data. *Marine*

865 *Ecology Progress Series*, 272, p.59-68.

866

867 Subramaniam A, Carpenter EJ and Falkowski PG (1999) Bio-optical properties of the

868 marine diazotrophic cyanobacteria *Trichodesmium* spp. II. A reflectance model for

869 remote sensing. *Limnol. Oceanogr* 44:618–627

870

871 Subramaniam A, Brown CW, Hood RR, Carpenter EJ and Capone DC (2002) Detecting

872 *Trichodesmium* blooms in SeaWiFS imagery. *Deep-Sea Res II* 49:107-121

873

874 Tomlinson MC, Stumpf RP, Ranisbrahmanakul V, Truby EW and others (2004)

875 Evaluation of the use of SeaWiFS imagery for detecting *Karenia brevis* harmful algal

876 blooms in the eastern Gulf of Mexico. *Remote Sens Environ* 91: 293–303

877

878 Tomlinson MC, Wynne TT, Stumpf RP. (2009) An evaluation of remote sensing

879 techniques for enhanced detection of the toxic dinoflagellate, *Karenia brevis*. *Remote*

880 *Sens Environ* 113:598–609.

881

882 Townsend DW, Pettigrew NR and Thomas AC (2001) Offshore blooms of the red tide

883 organism, *Alexandrium* sp., in the Gulf of Maine. *Continental Shelf Research* 21: 347-

884 369

885

886 Townsend DW, Pettigrew NR and Thomas AC (2005) On the nature of *Alexandrium*
887 *fundyense* blooms in the Gulf of Maine. *Deep Sea Research II*, 52: 2603-2630

888

889 Townsend DW, Thomas MA, McGillicuddy DJ and Rebeck NR (2014) Nutrients and
890 water masses in the Gulf of Maine - Georges Bank region: Variability and importance to
891 blooms of the toxic dinoflagellate *Alexandrium fundyense*. *Deep Sea Research II*. 103:
892 238-263

893

894 Vahtera E, Crespo BG, McGillicuddy Jr DJ, Olli K, and Anderson DM (2014)
895 *Alexandrium fundyense* cyst viability and germling survival in light vs. dark at a constant
896 low temperature. *Deep-Sea Res* 103:112-119

897

898 Vargas M, Brown CW, Sapiano MRP (2009) Phenology of marine phytoplankton from
899 satellite ocean color measurements. *Geophys. Res Lett.*36, L01608, doi:
900 10.1029/2008GL036006

901

902 White AW (1977) Recurrence of kills of Atlantic herring (*Clupea harengus harengus*)
903 caused by dinoflagellate toxins transferred through herbivorous zooplankton. *J Fish Res*
904 *Bd Can* 37(12):2262-2265

905

906 White AW (1980) Recurrence of kills of Atlantic herring (*Clupea harengus harengus*)
907 caused by dinoflagellates toxins transferred through herbivorous zooplankton. J Fish Res
908 Bd Can 37(12):2262-2265
909

910 List of Figure Captions:

911

912 Figure 1: Sampling stations in the Bay of Fundy, eastern Canada: The Wolves and off
913 shore stations 46 and 57.

914

915 Figure 2: Composite (24-31 May 2006) image of the Bay of Fundy showing the
916 probability of occurrence of diatoms derived from the SeaWiFS sensor and sea-surface
917 temperature (SST) derived from the AVHRR sensor for the same period, and same
918 location. Occurrence of diatoms is given as a percentage probability (0 – 100) of finding
919 diatom-dominated populations in that area during that time interval.

920

921 Figure 3: Schematic of the satellite-based warning system that relies on two SST
922 thresholds and one PDO threshold to infer safe, non-conclusive and toxic level of *A.*
923 *fundyense*.

924

925 Figure 4: Eight-day climatology (1998-2007) of satellite-derived SST (red diamonds),
926 probability of occurrence of diatoms (blue triangles), chlorophyll-a concentration (green
927 squares) and wind speed and direction, as well as in situ cell abundance of *A. fundyense*
928 (black Circle) in the Bay of Fundy (Wolves station).

929

930 Figure 5: Eight-day climatology (1998-2007) and range of variation of a) satellite-derived
931 SST, b) probability of occurrence of diatom and c) in situ cell abundance of *A. fundyense*
932 at the Wolves station.

933

934 Figure 6: *A. fundyense* cell abundance as a function of SST and probability of diatom
935 occurrence using the development dataset. Warning alerts (threshold 1 to 3) are colour-

936 coded from green, to orange to red for low, inconclusive and high risk of toxicity,
937 respectively.

938

939 Figure 7: Performance score of the warning algorithm as a function of a) lower threshold
940 of sea-surface temperature (SST_{LT}), b) upper threshold of sea-surface temperature
941 (SST_{UT}) and c) threshold of probability of occurrence of diatom (PDO_T).

942

943 Figure 8: *A. fundyense* cell abundance as a function of time at station Wolves (a), station
944 57 (b) and station 46 (c) for the year 2011. Solid circles are color-coded as a function of
945 satellite warning level, i.e., green, orange and red for low, inconclusive and high risk of
946 toxic level of *A. fundyense* cell abundance respectively.

947

948 Figure 9: Eight-day composite image of *A. fundyense* warning system for the entire Bay
949 of Fundy from the 22 April to 7 July 2011. The color-coding represents low (green ≤ 150
950 $\text{cells}\cdot\text{L}^{-1}$), medium (orange, inconclusive information on *A. fundyense* toxicity level) and
951 high ($>150 \text{ cells}\cdot\text{L}^{-1}$) *A. fundyense* cell abundance. Numbers in boxes indicate the cell
952 abundance of *A. fundyense* at the Wolves station (black solid star).